Polymer 50 (2009) 3698–3705

Contents lists available at ScienceDirect

Polymer

journal homepage: www.elsevier.com/locate/polymer

Preparation and characterization of polylactide/thermoplastic konjac glucomannan blends

Changgang Xu, Xuegang Luo*, Xiaoyan Lin, Xiurong Zhuo, Lili Liang

School of Material Science and Engineering, Southwest University of Science and Technology, Mianyang, Sichuan 621010, People's Republic of China

ARTICLE INFO

Article history:
Received 5 November 2008
Received in revised form
18 May 2009
Accepted 4 June 2009
Available online 10 June 2009

Keywords:
Thermoplastic konjac glucomannan
Polylactide
Blending

ABSTRACT

In this article, a new degradable thermoplastic konjac glucomannan (TKGM) was synthesized by graft copolymerization of vinyl acetate and methyl acrylate onto konjac glucomannan (KGM). Melt blending of polylactide (PLA) and TKGM has been performed in an effort to improve the processing and comprehensive mechanical properties of PLA and TKGM without compromising its degradability and biocompatibility. The miscibility, processing rheology, phase morphology, thermal properties, interaction, crystallization and mechanical properties of PLA/TKGM blends were investigated in detail. The thermal processing property of PLA/TKGM blend (60/40) was quite close to low density polyethylene (LDPE). As observed from the tan δ curves in dynamic mechanical analysis, all of the blends exhibit a single glass transition over the entire composition range, indicating that the blends were thermodynamically miscible. The TKGM exhibited a relatively broad endothermic peak at around 120 °C, which was lower than that of KGM. And an obvious glass-transition behavior was obtained around 26.6 °C. Furthermore, the PLA/TKGM blend (60/40) had a very high elongation at break of 234.8%, while the tensile strength remained as high as 36.5 MPa. And the PLA/TKGM blend (20/80) resulted in an even greater ductility with an elongation at break of 520.5% as compared with 14.1% for pure PLA. A substantial increase in the non-notched impact strength was also observed with the PLA/TKGM blend (20/80) demonstrating two times the impact strength of pure PLA.

1. Introduction

Blending of polymers is an effective alternative way to acquire new materials with desired properties without having to synthesize totally new materials. Other advantages for polymer blending are versatility, simplicity, and inexpensiveness [1]. Nowadays, natural polymeric materials have become increasingly important due to potential limitation of petroleum resources as well as increasingly environmental concerns. Biodegradable polymers such as polylactide (PLA), poly(ε-caprolactone) (PCL), poly(β-hydroxybutyrate) (PHB) and poly(propylene carbonate) (PPC), which were improved by these renewable and natural resources including starch, cellulose and wood flour have attracted much attention.

Polylactide (PLA), a biodegradable polymer which can also be produced from annually renewable resources, has gained recently a growing attention. However, PLA is not widely used because of its intrinsic brittleness [2], high cost as compared with synthetic plastics [3]. And its comprehensive mechanical properties, especially elongation at break and impact strength, could not meet the use requirement. In order to modify various properties or to reduce the cost, many researches on PLA blends with other polymers have been carried out [4–9]. But most of these blends are immiscible and non-degradable, which clearly limits the biomedical applications of the prepared blends. So blending of PLA with other biodegradable polymers, such as poly(butylenes succinate) [10], soy protein [11], poly(hydroxy ester ether) [12], thermoplastic starch [13], hexanoyl chitosan (H-chitosan) [1], poly(vinyl acetate-co-vinyl alcohol) [14], poly(β-hydroxybutyrate) [15], hyaluronic acid [3], poly(glycolide) [16], poly(ether)urethane elastomer [17] and polyamide elastomer [18], to produce fully degradable hybrids with good mechanical properties had been studied but the miscibility of most of the blends were the biggest problem either.

Contrarily to PLA, konjac glucomannan (KGM), one of the oldest and richest natural polymer on earth, can be obtained to yield various useful products. It is a copolymer of β-(1 → 4) linked D-glucose and D-mannose in the molar ratio of 1:1.6 with a low degree of acetyl groups (approximately 1 acetyl group per 17 residues) at the C-6 position [19,20]. Because of a lot of very active primary hydroxyl $-CH_2OH$ at the C-6 position of every constitutional unit, many

* Corresponding author. Tel./fax: +86 0816 6089009.
E-mail address: lxg@swust.edu.cn (X. Luo).

0032-3861/$ – see front matter © 2009 Elsevier Ltd. All rights reserved.
doi:10.1016/j.polymer.2009.06.007

chemical reactions can happen at this position, such as esterification, etherification, nitration [21] and graft polymerization [22]. The research on KGM so far has been limited to the isolation and characterization of the solution and bulk properties and the gelling behavior, mainly for food applications [23,24]. In addition, KGM can be extruded into films for coatings and packaging applications. A major problem concerning the thermal processing of polysaccharides is the strong interchain interactions which exist due to extensive hydrogen bonding. These interactions result in a polymer system which typically undergoes thermal decomposition before reaching its melting point [25]. KGM is a natural polymer material but with poor mechanical properties, water resistance and anti-aging properties, of which the process of material melts plastification is difficult. So the thermoplastic modification and application development of KGM are limited. Moreover, KGM has some other drawback, it being incompatible in blending and copolymerization only in the presence of strengthening agent and filling agent of low content in composite polymer, which has not much significance in the using of plentiful biological nature resources.

A novel thermoplastic material called thermoplastic konjac glucomannan (TKGM), which is a water resistant material, is thought to possess good thermoplasticity and biocompatibility. It is synthesized from KGM, vinyl acetate (VAc) and methyl acrylate (MA) by graft copolymerization in the laboratory. Meanwhile, the crystalline structure of the semi-crystalline KGM was broken down and rendered it completely amorphous. The TKGM is thermoplastic and hydrophobic. However, the TKGM cannot be widely used for plastic extruding, blow molding, injection molding and foaming because of the low tensile strength and poor processing characteristics. Once the TKGM is properly plasticized and modified, the TKGM can flow just as any synthetic polymer and is therefore suited for conventional molding and extrusion technologies.

In this paper, a new thermoplastic material (TKGM) was prepared and characterized. The blending of PLA/TKGM was firstly investigated. The PLA/TKGM blends were focused on reducing the cost of the material and improving the processing and comprehensive mechanical properties of PLA and TKGM. The miscibility and phase behavior of PLA/TKGM blends were studied, whilst the change of structure for the blends was characterized by FTIR. The thermoplastic process properties of PLA/TKGM blends were evaluated by comparing with LDPE. Meanwhile, this study was to precisely understand the different thermal properties of PLA/TKGM blends synthetically using differential scanning calorimetry (DSC). Additionally, the crystallization of the blends was tested by X-ray diffraction (XRD).

2. Experimental part

2.1. Materials and sample preparation

All chemical reagents used were obtained from commercial sources in Mianyang, China. And all are of analytical grade. The KGM sample with a number average molecular weight of 800,000 was a gift from Mianyang Konjac Co. Ltd. (Sichuan, China). Polylactide (PLA), blow molding grade, was provided by Shenzhen Brightchina Industrial Co. Ltd. It has a number average molecular weight of 100,000. PLA was dried at 65 °C for at least 8 h.

Thermoplastic konjac glucomannan (TKGM) was synthesized from konjac glucomannan (KGM), vinyl acetate (VAc) and methyl acrylate (MA) by inputting 3.0 g of KGM and 200 ml of water into a four-necked round bottom flask equipped with stirrer, thermometer, nitrogen gas inlet and condenser, agitating for 30 min at 80 °C. Until KGM had been gelatinized (KGM slurry turned to a transparent solution), the flask contents were cooled to 70 °C. The monomers including VAc (4.8 g) and MA (7.2 g) were added in drops within 10 min after ammonium persulfate (APS) having been added, and then the mixture was allowed to react for 3 h at 75 °C. The graft copolymer product was separated by filtration and then the liquid was fetched into a beaker fitted with ethanol after the reaction, and finally freeze dried to give TKGM.

The blends of PLA and TKGM with different mixing mass ratios [100/0, 80/20, 60/40, 50/50, 40/60, 20/80, 0/100] coded as PLA, PT1, PT2, PT3, PT4, PT5 and TKGM were produced for 15 min in an internal mixer of XSS-300 torque rheometer which made in Shanghai Kechuang Machinery Co. Ltd, The internal mixer was controlled steadily at a temperature of 180 ± 2 °C and a rotation rate at 40 rev min^{-1}.

2.2. The viscosity of the KGM solution

The viscosity of the KGM solution was measured by a HAAKE instrument RS6000 rotary rheometer. The measurements were performed at 75 °C and a shear rate of 10^{-6} s^{-1} using 60 mm diameter cone-plate (cone angle 1°).

2.3. The water absorption of the TKGM

The water absorption of TKGM was performed at room temperature on injection molded according to the GB/T 1034-1998 method. The percentage of water absorption (w_m) was calculated by the following equation:

$$w_m = \frac{m_2 - m_1}{m_1} \times 100\% \quad (1)$$

m_1, m_2 in Eq. (1) are the weight of the TKGM without immersion and after 24 h immersion, respectively.

2.4. Dynamic mechanical analysis

Dynamic mechanical analysis (DMA) was carried out with a TA Instruments Q800 DMA in the single cantilever mode. The dynamic loss ($\tan\delta$) was determined at a frequency of 1 Hz and a heating rate of 3 °C/min as a function of temperature from −20 °C to 150 °C.

2.5. Microscopic analysis

The morphology of PLA/TKGM blends was investigated by SEM (S440 Leica Cambridge LTD.) from the appearance of the fracture surfaces. All specimens were sputter coated with gold prior to examination.

2.6. Differential scanning calorimetry

The heating and cooling DSC curves of the blends were determined on a TA Instruments Q200 DSC. Temperature and heat of fusion are calibrated with indium, the heat capacity being calibrated with a sapphire sample. For all experiments, the purge gas is nitrogen (50 ml/min). The measurements were made using 3.50 ± 0.50 mg samples. The samples were heated from 0 to 180 °C at a heating rate of 20 °C/min (the first heating scan). Then the samples were quenched, heated from 0 to 180 °C (the second heating scan). The glass-transition temperature (T_g), cold-crystallization temperature (T_c) and the melting temperature (T_m) were measured as the temperature corresponding to the midpoint of the heat capacity increment. The measurement of isothermal crystallization was taken at 100 °C.

2.7. Fourier transform infrared spectroscopy

Fourier transform infrared spectra of the KGM and PLA/TKGM blends were determined on a Nicolet 6700 FTIR spectrometer with an OMNIC-sampler in the range 675–4000 cm^{-1}.

2.8. X-ray diffraction

The materials were mounted directly in the sample holder. The X-ray diffraction (XRD) curves of the materials were recorded with an X' Pert PRO (Holand) X-ray diffractometer and used a CuKα target at 40 kV and 40 mA. The diffraction angle ranged from 3° to 35°.

2.9. Mechanical properties

All the mechanical property measurements were performed on injection molded blends. Tensile strength and elongation at break were measured on a mechanical tensile tester (CMT6104-SANS, China), according to the GB/T 1040-92 method at 25 °C and 50% relative humidity. The samples were injection molded standard type dumbbell-shaped samples with a thickness of 3.0 ± 0.1 mm. A crosshead speed of 5 mm/min was used. Five specimens were used for each blend condition.

The non-notched impact tests were carried out using a standard impact tester (XJJ-50, China) at 20 °C and 50% relative humidity. The samples were injection molded standard type plate samples with a thickness of 3.0 ± 0.1 mm, a width of 14 ± 0.1 mm. The span length is 60 mm. At least five specimens were tested for each sample to get an average value.

$$a_k = \frac{A_k}{bh_k} \quad (2)$$

A_k, b, h_k, a_k in Eq. (2) are the impact energy, width, thickness and impact, separately.

3. Result and discussion

3.1. Synthesis and FTIR analysis of thermoplastic konjac glucomannan

Graft copolymerization of VAc and MA onto KGM was performed by free-radical polymerization using APS as initiator. Ammonium persulfate can effectively initiate saccharide units to generate free-radical sites, which react with VAc and MA monomers to form graft copolymer. The chemical structure of KGM is shown in Scheme 1. The TKGM was obtained and the formation is shown in Scheme 2. As initiated by APS, the viscosity of the KGM solution decreased from 4.59×10^8 to 7.58×10^6 mPa s. The water absorption of TKGM was only 3.8%.

FTIR is of importance in the study of the molecular structure. The width and intensity of the spectrum bands, as well as the position of the peaks, are all sensitive to environmental changes and to the conformations of macromolecules at the molecular level. From IR spectrum of KGM (Fig. 1), it can be seen that the absorption band of the stretching of –OH groups was at 3373 cm^{-1} and the band at 2921 cm^{-1} predominantly arose from C–H asymmetric stretching in the methylenes. The characteristic absorption bands of the mannose in the KGM appeared at 875 and 808 cm^{-1}. The peak at 1727 cm^{-1} was dominated by the stretching of the C=O in the carbonyl of acetyl groups. The peak at 1635 cm^{-1} was attributed to the C–O in the intermolecular hydroxy groups. The adsorption peak at 1062 cm^{-1} provided the evidence of the characteristic absorption band of C6–OH. The band at 1027 cm^{-1} was characteristic absorption of bridge O stretch.

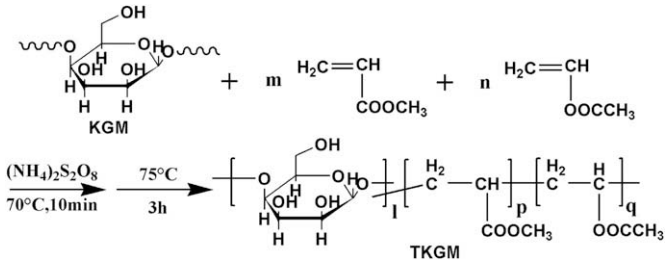

Scheme 2. Preparation of the TKGM.

In the spectra of TKGM, the disappearance of peaks at 1062 cm^{-1}, 1635 cm^{-1} and 3373 cm^{-1} was due to the reason that the –OH groups of the KGM reacted with MA and VAc. As compared with the FTIR spectrum of KGM, the peaks at 1089 cm^{-1} and 1164 cm^{-1} in TKGM were from the C–O stretching of C6–O– which formed by graft copolymerization and the C–O stretching of $-COOCH_3$ in MA, respectively. It can be seen that the C–H bending at 1444 cm^{-1} and symmetric stretching at 2852 cm^{-1} of the $-CH_2-$ bands were enhanced in the TKGM, indicating the KGM having grafted with MA and VAc or the polymerization of the MA and VAc. In addition, peak at 1027 cm^{-1} of the characteristic absorption band of bridge O stretch was weakened. This observation confirmed that the KGM was degraded by APS to form the free radicals. Moreover, in contrast with the spectrum of KGM, the peak of C=O stretching in the TKGM was enhanced and shifted to 1735 cm^{-1}. It was found that the peak arose from the C–O stretching of VAc was shifted from 1250 to 1236 cm^{-1} in the TKGM. This result provided strong evidence supporting the grafting MA and VAc onto the KGM as well as the hydrogen bonding decreased [26]. It was also found that characteristic absorption band of the mannose at 808 cm^{-1} was shifted to 827 cm^{-1}, suggesting that the crystalline structure of KGM was destroyed.

3.2. Torque measurements

The variation of torque with blending time for PLA/TKGM blends is presented in Fig. 2. It was obvious that TKGM exhibited a slow not

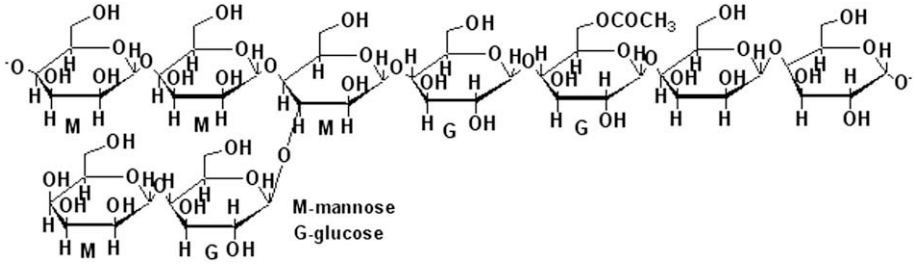

Scheme 1. Chemical structure of konjac glucomannan.

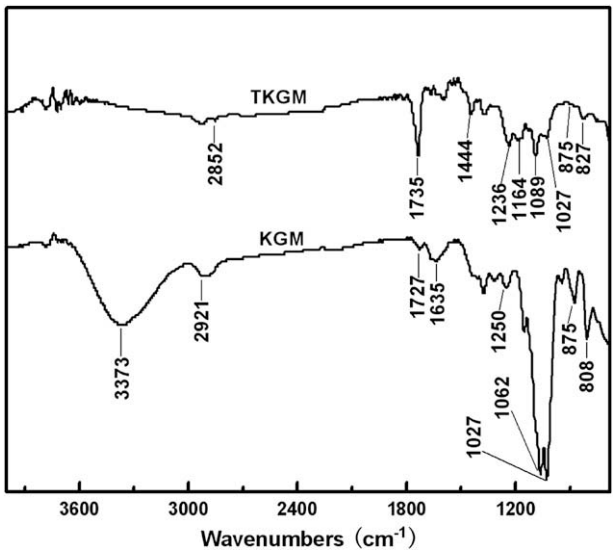

Fig. 1. FTIR spectra of KGM and TKGM.

a sharp decrease curve in comparison to PLA. The torque value of TKGM approached a stable value fluctuating around 9.8 N m when the blending time was greater than 250 s, suggesting that the plasticizing rate of TKGM was slow and the good plasticizing had occurred after about 250 s. Moreover, with the increasing of PLA, the descending rate of the torque curves increased, but the equilibrium torque decreased sharply. It may be suggested that the viscosity of PLA/TKGM blends was lower than that of TKGM.

In order to evaluate the thermoplastic process properties of PLA/TKGM blends, LDPE was used as the reference standard because of its good thermoplastic process properties. It was found that equilibrium torque and plasticizing time for LDPE were 5.0 N m and 40 s, respectively. As compared with LDPE, pure PLA had the longer plasticizing time and much lower equilibrium torque, suggesting that the melt strength was low for PLA. However, with comparison between LDPE and PLA/TKGM blends, the torque curve of sample PT2 was quite close to LDPE, having equilibrium torque of 4.8 N m and plasticizing time of 60 s. Based on the above results, one can infer that the PLA blending with TKGM not only improve the melt processing properties of TKGM, but also enhance the melt strength of PLA.

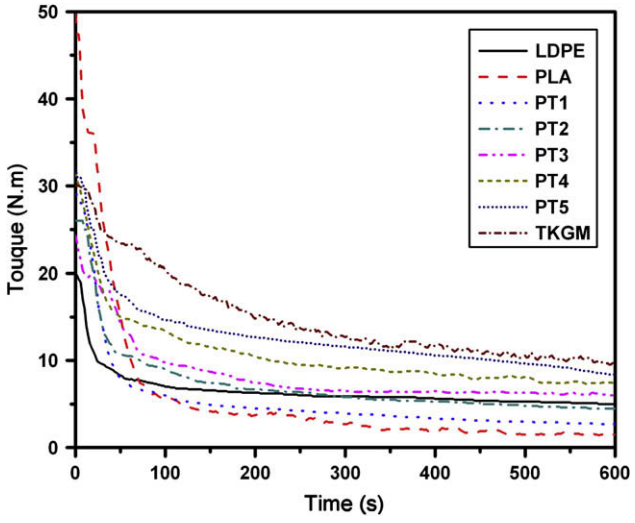

Fig. 2. Torque curves of LDPE and PLA/TKGM blends.

3.3. Miscibility and morphology of PLA/TKGM blends

The dynamic mechanical properties of PLA/TKGM blends were measured and used to evaluate the compatibility of blend. Fig. 3 shows dynamic viscoelastic curves for neat PLA, PT2, PT4 and neat TKGM. In Fig. 3(a), the storage modulus (E') of neat PLA dropped abruptly, at around 70 °C, due to the glass transition. The E' at around 60 °C for PLA/TKGM blends gradually decreased with TKGM content increasing and then rose at around 100 °C because of the cold crystallization of PLA. The starting cold crystallization temperature of the PLA shifted to a lower degree with the addition of TKGM may be due to the enhancement in cold-crystallization ability of PLA with the incorporation of TKGM.

A single composition-dependent T_g is the criterion commonly used for determining the miscibility of a polymer blend. PLA has indeed been reported to be miscible with some polyether, such as PEO and PPG [6,27]. Fig. 3(b) shows variations of the loss tangent (tan δ) with temperature for the PLA/TKGM blends, and the result

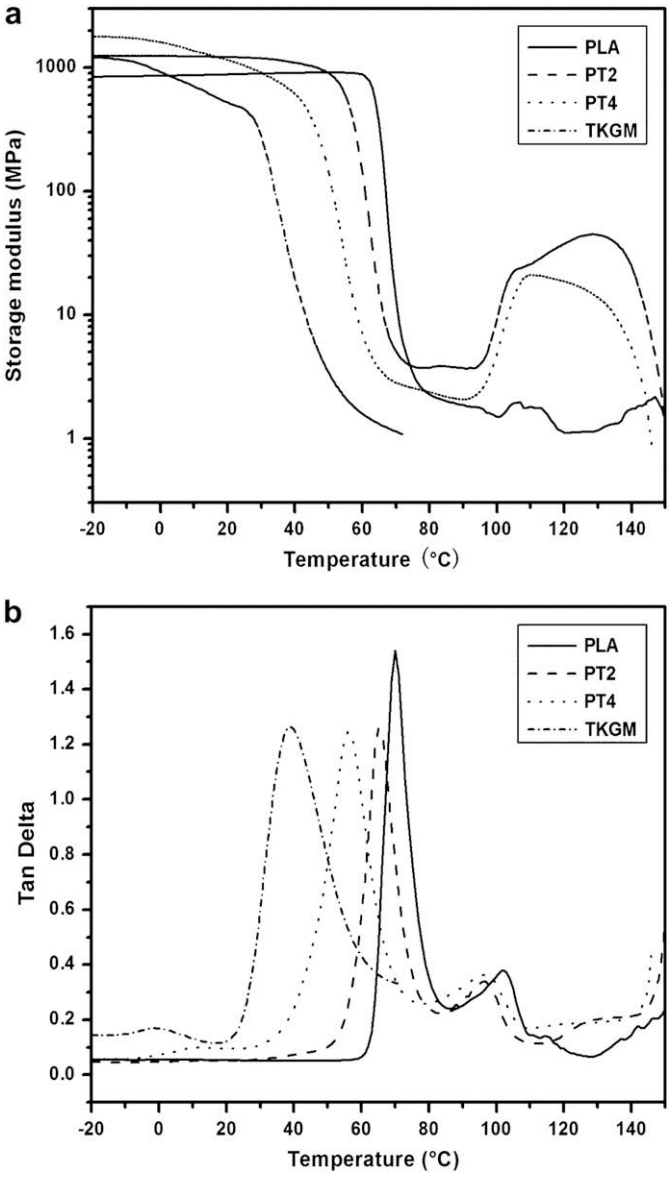

Fig. 3. Dynamic viscoelastic curves for PLA/TKGM blends: (a) storage modulus versus temperature curves (b) tan δ versus temperature curves.

Table 1
Thermal characteristics of KGM and PLA/TKGM blends.

Samples	T_g[a] (°C)	T_g[b] (°C)	T_g[c] (°C)	T_c (°C)	ΔH_c (J/g)	T_m (°C)	ΔH_m (J/g)	Isothermal peak (min)
PLA	70.1	64.1	61.4	132.0	9.3	151.5	6.9	5.0
PT1	67.6	51.8	57.2	141.1	0.2	151.4	0.4	4.0
PT2	65.3	45.3	47.7	135.4	0.4	150.8	1.1	2.5
PT3	60.1	40.6	44.2	130.0	1.1	149.9	3.6	2.3
PT4	56.1	33.1	40.1	–	–	149.1	0.2	–
PT5	52.2	31.0	36.2	–	–	147.6	0.3	–
TKGM	38.7	25.1	29.5	–	–	–	–	–
KGM	–	–	–	–	–	–	–	–

[a] From DMA instrument.
[b] In first heating curves.
[c] In second heating curves.

showed that the tan δ increased sharply at a particular temperature, while the onset of segmental motion started [28]. In the case of PLA/TKGM blends, the tan δ peak generally broadened and decreased in intensity with an increasing TKGM content. The glass transition temperatures (T_g) were calculated from the tan δ peak temperature, summarized in Table 1. As observed from the tan δ curves, all of the blends showed a single glass transition temperature, indicating that the blends were thermodynamically miscible and there were some molecular interactions between the two components. In the TKGM molecules, the polyether was the soft segment and the mannose acts as the hard segment. The soft segment played an important role in enhancing the compatibility between PLA and TKGM molecules [18].

Fig. 4 shows the SEM micrographs of the PLA/TKGM blends. The compatibility of two kinds of polymer could be evaluated from the degrees of homogeneity and the compactness of the blends. In general, PLA/TKGM blends displayed smooth surfaces, indicating that the blend formed a homogeneous mixture. Although the cross-section morphologies of the blends exhibited a little lamellar structure, there was no obvious phase separation. It is concluded, therefore, that the good interfacial interactions occurred between PLA and TKGM.

3.4. Thermal behaviors of PLA/TKGM blends

The DSC curves obtained for neat KGM and PLA/TKGM blends are illustrated in Fig. 5. The results obtained are summarized in Table 1. In the 1st heating curves, the original KGM sample showed a sole endothermic peak at 130 °C. It may be due to a loss of hydroxyl group of KGM as water molecules [29]. The KGM–H_2O crystallite formed by hydrogen bonds was destroyed. The reaction was as follows: KGM–H_2O → KGM + H_2O. On the other hand, the TKGM obtained after graft copolymerization exhibited a relatively broad endothermic peak at around 120 °C, which was lower than that of KGM. The most interesting here was that an obvious glass-transition behavior obtained around 26.6 °C, indicating that the intermolecular hydrogen bonding interactions decreased as discussed in FTIR.

The compatibility of PLA with the TKGM was proved once more that the T_gs decreased with the increasing TKGM content and only a single T_g was obtained, which was consistent with the DMA results. However, the T_g value obtained from DSC was lower than that of DMA, which can be attributed to the different measuring mechanisms for DMA and DSC [30].

Once TKGM was added into the blends, obvious changes in the thermal properties appeared. From Fig. 5(A), the PLA showed a sole cold-crystallization peak at 130 °C, followed by the crystal fusion at around 150 °C. It is noticed that the PT1 showed a slight cold-crystallization peak at around 141 °C. With the TKGM content further increasing, the cold-crystallization enthalpy (ΔH_c) and the melting enthalpy (ΔH_m) had a tendency of increasing until more than 50% TKGM was added. Meanwhile, the melting point of the blends decreased with the increasing of TKGM content.

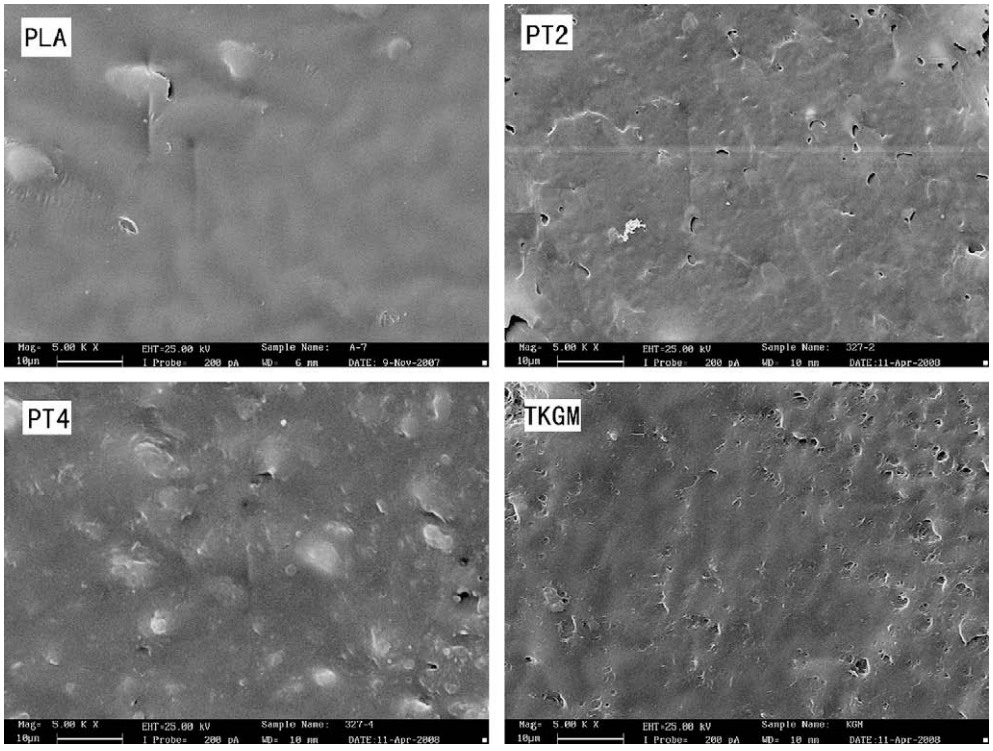

Fig. 4. SEM micrographs (×5000) of cross-section for PLA, PT2, PT4 and TKGM.

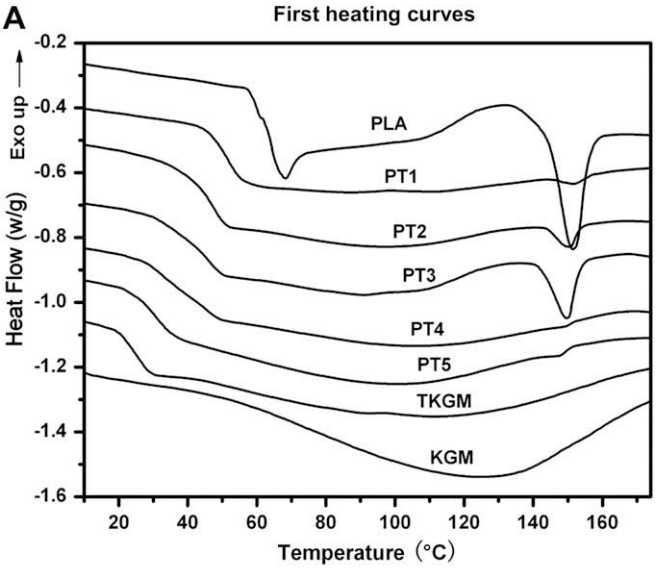

Fig. 5. DSC curves (A, B) of KGM and PLA/TKGM blends.

In the case of PLA/TKGM blends, the endothermic peak at about 120 °C generally broadened and shifted to lower temperature with an increasing TKGM content. The results showed that the different TKGM content adding had effect on the thermal properties of PLA due to the flexible chain of TKGM originated from MA and VAc. Furthermore, the short chain segments methylenes which had great influence on the motion of main chain increased and affected the crystallization of the blends. In the second heating curves which were melt-quenched after the first heating of the samples, shown in Fig. 5(B), we observed that the PLA showed a slender melting peak at 150 °C, as compared with the others. Therefore, the endothermic peaks of the others in the first heating curves were not reversible, which may be due to the water loss.

In Fig. 6, isothermal melt crystallization of KGM and PLA/TKGM blends was investigated at 100 °C. As can be seen, the sample of PLA exhibited a broad exothermic peak at 5.0 min and its crystallization time was about 45 min. This result showed that PLA had a slow rate of crystallization at 100 °C. As the TKGM was added, the crystallization rates of all samples were changed. In fact, with less than 50% TKGM increasing, the exothermic peaks narrowed gradually and

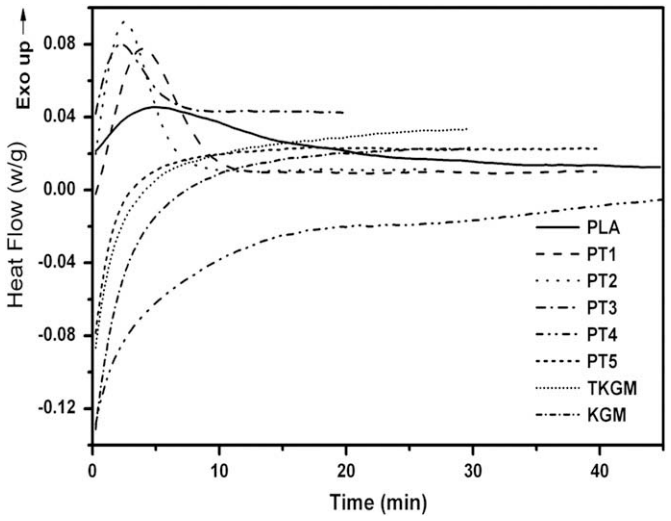

Fig. 6. Isothermal melt crystallization curves of KGM and PLA/TKGM blends at 100 °C.

shifted to left. It is therefore known that the crystallization rate was enhanced with the TKGM compositions increasing. However, similar to the isothermal curve of KGM, the blends with more than 50% TKGM content, such as PT4, PT5 and TKGM, showed no sharp crystallization exothermic peaks.

3.5. FTIR analysis of the PLA/TKGM blends

Intermolecular interactions occur when different polymers are compatible. So the FTIR spectra of the blends are different from those of pure polymers, which can be used to the study of the extent of polymer compatibility. The FTIR spectra of PLA, TKGM and PT3 are shown in Fig. 7. It can be seen that peak of PLA at 1755 cm^{-1} assigned to C=O stretching, as well as C=O stretching at 1735 cm^{-1} in TKGM, shifted to 1747 cm^{-1} in PT3. In addition, a large broad band of the C–C stretching at 1188 cm^{-1} in PT3 could be observed. The results suggested that the specific interactions between PLA and TKGM were formed [31]. This may account for miscibility of PLA and TKGM.

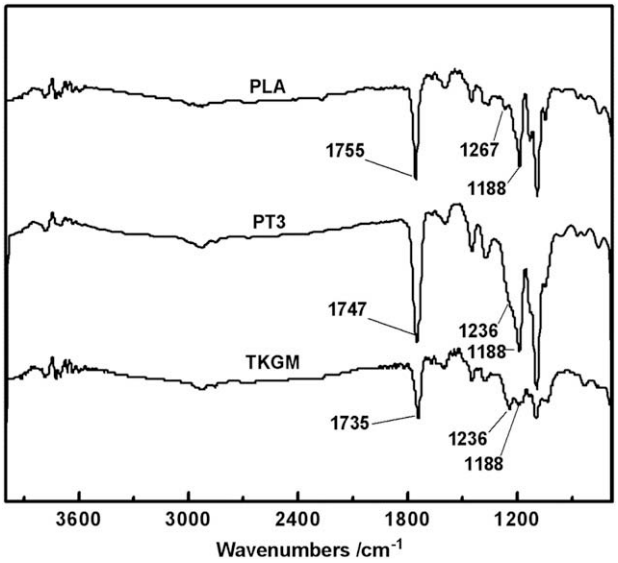

Fig. 7. FTIR spectra of PLA, PT3 and TKGM.

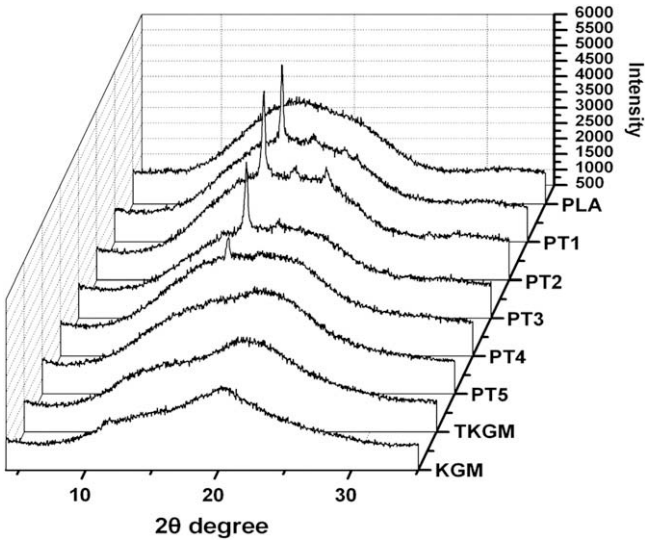

Fig. 8. XRD curves of KGM and PLA/TKGM the blends.

3.6. XRD Analysis of the PLA/TKGM Blends

XRD patterns for pure KGM and the PLA/TKGM blends are illustrated in Fig. 8. The XRD pattern of KGM showed a weak but broad reflection falling at about 2θ of around 21°. For TKGM, peak at 2θ of around 21° became broader, indicating that the integrity of the KGM crystal form was reduced owing to the conjugation of KGM with MA and VAc. And for pure PLA, the obtained XRD pattern showed one broad diffraction peak centering at the 2θ of around 17°. When crystallizing in a pseudo-orthorhombic unit cell (with axes $a = 1.07$ nm, $b = 0.595$ nm, and $c = 2.78$ nm), PLA should show main diffraction peaks at the 2θ of 15, 17 and 19° [32]. Obviously, with the increase of TKGM, blends showed sharp diffraction peaks at the 2θ of around 17° except for sample PT5. One sharp diffraction peak at the 2θ of around 19° can be found for sample PT1, PT2 and PT3, but diffraction peak at the 2θ of around 21° only appeared for sample PT2. The diffraction patterns for PLA/TKGM blends appeared in the characteristic diffraction peaks of both pure PLA and TKGM. It was suggested that the presence of one component affected the ordered structure which would be observed for the other component.

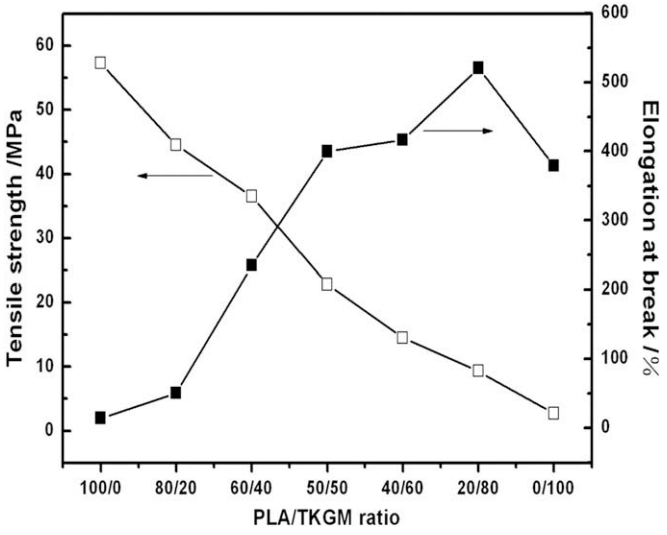

Fig. 9. Tensile strength and elongation at break of PLA/TKGM blends.

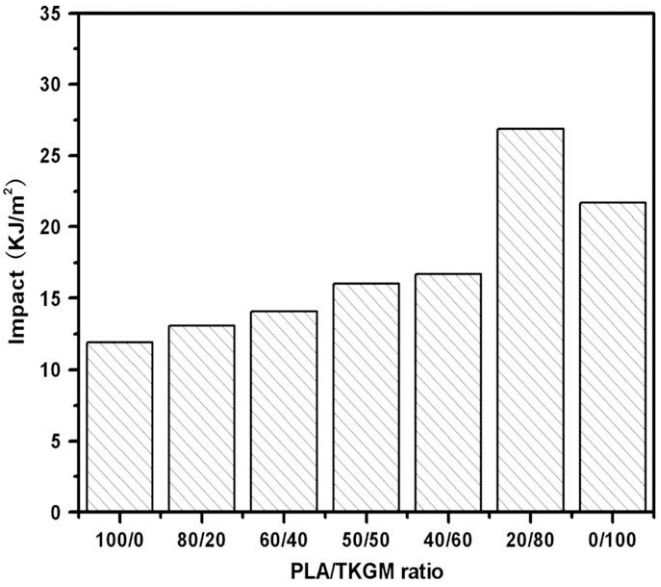

Fig. 10. Impact strength of PLA/TKGM blends.

3.7. Mechanical properties of the PLA/TKGM Blends

The tensile behavior of the PLA/TKGM blends is shown in Fig. 9. Neat PLA is very rigid and brittle. The tensile strength for PLA is 57.1 MPa; whereas the elongation at break is only about 14.1%. For PLA/TKGM blends, the tensile strength decreased continuously but the elongation at break increased as TKGM content increasing. It was very interesting to find that the blend with 60 wt% PLA had a very high elongation at break of 234.8%, while the tensile strength remained as high as 36.5 MPa. When the PLA content is more than 50 wt% in the blends, the tensile strength of the blends is greater than 20 MPa. It was also found that the PLA/TKGM blend (20/80) had a maximum elongation at break of 520.5%.

The impact strength of the PLA/TKGM blends was also measured for various TKGM contents, as shown in Fig. 10. An increase in the TKGM content resulted in a gradual increase in toughness. The impact strength was significantly changed from 11.9 KJ m^{-2} for neat PLA to 26.9 KJ m^{-2} for the PLA/TKGM blend (20/80). The mechanical properties for the PLA/KGM blends clearly indicated a synergistic effect that exceeds the results obtained for any single component.

4. Conclusions

A new thermoplastic material (TKGM) with 3.8% water absorption ratio was prepared and characterized. IR spectroscopy of the TKGM reveals that the grafting of MA and VAc unto KGM occurred. The hydrogen bonding decreased and an obvious glass-transition behavior was obtained in TKGM.

PLA/TKGM blends were fabricated by melt mixing to prepare a degradable and biocompatible polymer blend with improving processing and comprehensive mechanical properties. The processing fluidity, miscibility, phase morphology, crystallization and the structure were investigated by means of torque rheometer, DMA, SEM, DSC, FTIR and XRD. The PLA blending with TKGM not only improve the melt processing properties of TKGM, but also enhance the melt strength of PLA. The thermal processing property of PLA/TKGM blend (60/40) was quite close to low density polyethylene (LDPE). DMA and SEM tests showed that PLA/TKGM is a miscible system with an one-phase morphology. DSC results revealed that the addition of TKGM changed the thermal properties

of the blends. Furthermore, the specific interactions between PLA and TKGM were formed. And the PLA/TKGM blends showed significantly increasing of elongation at break as well as impact strength, compared with neat PLA. This improvement was due to a more homogeneous blend and the good miscibility. Overall, the blend approach with PLA/TKGM is an interesting technique to expand the property range of PLA and KGM materials.

Acknowledgements

This work was supported by the Nature Science Foundation of China (Grant No. 29876017). Experiments were conducted at Sichuan Key Laboratory of Biomass Chemical Derivatives.

References

[1] Peesan M, Supaphol P, Rujiravanit R. Carbohydr Polym 2005;60(3):343–50.
[2] Huneault MA, Li Hongbo. Polymer 2007;48(1):270–80.
[3] Wu CSH, Liao T. Polymer 2005;46(23):10017–26.
[4] Reddy N, Nama D, Yang YQ. Polym Degrad Stab 2008;93(1):233–41.
[5] Pannu RK, Tanodekaew S, Li W, Collett JH, Attwood D, Booth C. Biomaterials 1999;20(15):1381–7.
[6] Nijenhuis AJ, Colstee E, Grijpma DW, Pennings AJ. Polymer 1996;37(26):5849–57.
[7] Gajria AM, Dave V, Gross RA, McCarthy SP. Polymer 1996;37(3):437–44.
[8] Sheth M, Kumar RA, Dave V, Gross RA, McCarthy SP. J Appl Polym Sci 1997;66(8):1495–505.
[9] Park JW, Im SS, Kim SH, Kim YH. Polym Eng Sci 2000;40(12):2539–50.
[10] Ikehara T, Nishikawa Y, Nishi T. Polymer 2003;44(21):6657–61.
[11] Zhang JW, Jiang L, Zhu LY. Biomacromolecules 2006;7(5):1551–61.
[12] Cao X, Mohamed A, Gordon SH, Willett JL, Sessa DJ. Thermochim Acta 2003; 406(1–2):115–27.
[13] Park JW, Im SS. Polymer 2003;44(15):4341–54.
[14] Zhang LL, Xiong CD, Deng XM. Polymer 1996;37(2):235–41.
[15] Huneault MA, Li HB. Polymer 2007;48(1):270–80.
[16] Sivalingam G, Madras G. Polym Degrad Stab 2004;84(3):393–8.
[17] Yongjin L, Hiroshi S. Macromol Biosci 2007;7:921–8.
[18] Zhang W, Chen L, Zhang Y. Polymer 2009;50:1311–5.
[19] Maeda M, Shimahara H, Sugiyama N. Agric Biol Chem 1980;44(2):245–52.
[20] Kaname K, Kohsaku O, Kenichi H. Carbohydr Polym 2003;53(2):183–9.
[21] Gao S, Zhang L. Macromolecules 2001;34(7):2202–7.
[22] Liu Z, Chen L, Zhou R. Polymer 2005;46(16):6274–81.
[23] Whistler RL, BeMiller JN. Industrial gums, polysaccharides and their derivatives, 3rd ed. London: Academic Press; 1993. p. 47.
[24] Nishinari K, Williams PA, Phillips GO. Food Hydrocolloids 1992;6(2):199–222.
[25] Xiao C, Lu Y, Zhang L. J Appl Polym Sci 2001(b);81(4):882–8.
[26] Chen JK, Kuo SW, Kao HC, Chang FC. Polymer 2005;46:2354–64.
[27] Piorkowska E, Kulinski Z, Galeski A, Masirek R. Polymer 2006;47(20):7178–88.
[28] Wu CS, Liao HT. Polymer 2007;48:4449–58.
[29] Pan ZD, He K, Wang YM. J Appl Polym Sci 2008;108:1566–73.
[30] Hatakeyama T, Quinn FX. Thermal analysis: fundamentals and applications to polymer science, 2nd ed.; 1994. New York.
[31] Tang T, Jing XB, Huang BT. J Macromol Sci Phys 1994;33:287–305.
[32] Kister G, Cassanas G, Vert M. Polymer 1998;39(2):267–73.